Inorg. Chem. **2006**, *45*, 8882–8886

Enhanced Near-Infrared–Luminescence in an Erbium Tetrafluoroterephthalate Framework

Banglin Chen,*,† Yu Yang,‡ Fatima Zapata,† Guodong Qian,*,‡ Yongshi Luo,§ Jiahua Zhang,§ and Emil B. Lobkovsky||

Department of Chemistry, University of Texas-Pan American, Edinburg, Texas 78541-2999, Department of Materials Science & Engineering, State Key Laboratory of Silicon Materials, Zhejiang University, Hangzhou 310027, People's Republic of China, Key Laboratory of Excited-State Processes, Changchun Institute of Optics, Fine Mechanics and Physics, China Academy of Science, Changchun 130021, People's Republic of China, and Baker Laboratory, Department of Chemistry and Chemical Biology, Cornell University, Ithaca, New York 14853-1301

Received April 4, 2006

Two erbium–organic frameworks $Er_2(BDC)_3(DMF)_2(H_2O)_2 \cdot H_2O$ (**1**) and $Er_2(BDC\text{-}F_4)_3(DMF)(H_2O) \cdot DMF$ (**2**) (BDC = 1,4-benzenedicarboxylate; BDC-F_4 = 2,3,5,6-tetrafluoro-1,4-benzenedicarboxylate or tetrafluoroterephthalate; DMF = dimethylformamide) have been synthesized and structurally characterized. Studies on thermal gravimetric analysis and the spectroscopic and luminescent properties of **1**, **2**, and their desolvated solid $Er_2(BDC)_3$ (**1a**) and partially desolvated solid $Er_2(BDC\text{-}F_4)_3(DMF) \cdot DMF$ (**2a**) indicate that fluorination can significantly improve the luminescence intensity of the Er ions by reducing the fluorescence quenching effect of the vibrational C–H bond; thus, the near-IR–luminescence intensity of **2a** is 3 times higher than that of **1a**.

Introduction

Metal−organic frameworks (MOFs) have been of extensive interest for their functional properties and thus potential applications in materials science. Self-assembly of metal ion and/or metal clusters with a variety of organic linkers has not only led to a unique type of porous materials for gas storage, separation, and catalysis but also produced a series of functional materials with special magnetism, nonlinear optics, and luminescence properties.[1,2] The research on luminescent MOF materials has been mainly focused on their UV−vis emission,[3] while emissive near-IR MOF materials have not yet been explored.[4]

To incorporate near-IR emissive metal sites such as Er^{3+}, Nd^{3+}, and Yb^{3+} into their MOF materials, we are particularly interested in tuning their functional properties for potential applications in sensing and optics.[5,6] The special advantage of such a MOF approach is to change the concentration of the emissive metal ions/unit volume systematically simply by incorporation of different organic linkers.[7] Species containing high-energy C−H, N−H, and/or O−H oscillators (normally existing in the ligands and solvents) significantly quench the metal excited states nonradiatively, leading to decreased luminescence intensities.[8] To reduce/eliminate such quenching effects, fully deuterated/fluorinated organic ligands have been incorporated into molecular organolanthanide compounds to enhance their luminescence intensities.[9−11] However, the effect of fluorination on the luminescence intensities of lanthanide−organic framework materials has not yet been examined. Herein we report the synthesis

* To whom correspondence should be addressed. E-mail: banglin@utpa.edu (B.C.), gdqian@zju.edu.cn (G.Q.).
† University of Texas−Pan American.
‡ Zhejiang University.
§ China Academy of Science.
|| Cornell University.

(1) Yaghi, O. M.; O'Keeffe, M.; Ockwig, N. W.; Chae, H. K.; Eddaoudi, M.; Kim, J. *Nature* **2003**, *423*, 705. Batten, S. R.; Robson, R. *Angew. Chem., Int. Ed.* **1998**, *37*, 1461. Kitagawa, S.; Kitaura, R.; Noro, S. *Angew. Chem., Int. Ed.* **2004**, *43*, 2334. Moulton, B.; Zaworotko, M. J. *Chem. Rev.* **2001**, *101*, 1629. Blake, A. J.; Champness, N. R.; Hubberstey, P.; Li, W. S.; Withersby, M. A.; Schroder, M. *Coord. Chem. Rev.* **1999**, *183*, 117. Kiang, Y. H.; Lee, S.; Xu, Z. T.; Choe, W. Y.; Gardner, G. B. *Adv. Mater.* **2000**, *12*, 767. Evans, O. R.; Lin, W. B. *Acc. Chem. Res.* **2002**, *35*, 511. Janiak, C. *Dalton Trans.* **2003**, 2781. Ferey, G.; Mellot-Draznieks, C.; Serre, C.; Millange, F. *Acc. Chem. Res.* **2005**, *38*, 217. Bradshaw, D.; Claridge, J. B.; Cussen, E. J.; Prior, T. J.; Rosseinsky, M. J. *Acc. Chem. Res.* **2005**, *38*, 273. Lin, W. B. *J. Solid State Chem.* **2005**, *178*, 2486. Kepert, C. J. *Chem. Commun.* **2006**, 695.

10.1021/ic060568u CCC: $33.50
Published on Web 09/27/2006

and crystal structures of two erbium−organic frameworks, $Er_2(BDC)_3(DMF)_2(H_2O)_2 \cdot H_2O$ (**1**) and $Er_2(BDC\text{-}F_4)_3(DMF)(H_2O) \cdot DMF$ (**2**) (BDC = 1,4-benzenedicarboxylate; BDC-F_4 = 2,3,5,6-tetrafluoro-1,4-benzenedicarboxylate or tetrafluoroterephathlate; DMF = dimethylformamide), and the near-IR−luminescence of the as-synthesized and activated compounds **1**, **2**, $Er_2(BDC)_3$ (**1a**), and $Er_2(BDC\text{-}F_4)_3(DMF) \cdot DMF$ (**2a**). The results demonstrate that the luminescence intensity of near-IR emissive MOFs can be significantly enhanced by incorporation of fluorinated organic linkers.

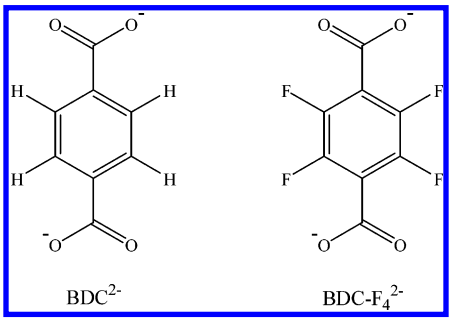

Experimental Section

Materials and Instrumentation. All reagents and solvents employed were commercially available and used as supplied without further purification. Powder X-ray diffraction (PXRD) diffractograms were measured with a Siemens D5005 X-ray diffractometer with a Cu Kα line (λ = 1.541 78 Å) as the incident beam. A Gobel mirror was employed as a monochromator. The sample powder was loaded into a glass holder and leveled with a glass slide before mounting it onto the sample chamber. The specimens were scanned between 4 and 40°. The scan step width was set to 0.01° and the scan rate to 0.01°/s. Thermal gravimetric analysis (TGA)−differential scanning calorimetry (DSC) data were obtained on a TGA G500 V5.3 Build 171 instrument with a heating rate of 10 °C/min under a N_2 atmosphere. The Fourier transform IR spectra were recorded by a Nicolet Avatar 360 spectrometer using KBr pellets. Solid samples of compounds **1** and **2** were employed to determine their UV−vis−near-IR absorption spectra, respectively. The UV−vis−near-IR absorption spectra of solid samples were determined by a Hitachi U-4100 spectrometer; the samples were deposited on glass substrates (Corning 2947) by a few drops of a sample−ethanol emulsion followed by the evaporation of ethanol before measurement and then measured by transmittance. Solid samples of compounds **1**, **2**, **1a**, and **2a** were used to determine their near-IR−photoluminescence spectra. The near-IR−photoluminescence spectra were determined at room temperature by using a spectrometer equipped with a monochromator (Spex 1269; SPEX Industries Inc., Edison, NJ) and a liquid-N_2-cooled Ge detector (EO-817L; Yellow River Systems Inc., USA), together with a 808-nm laser diode (LD) as the excitation source. The solid samples employed in near-IR−photoluminescence spectral measurements were in the form of tablets, which were fabricated in a cavity-like sample holder with the same amount of solids under the same pressure. The measuring geometry and focusing were kept unchanged during near-IR−photoluminescence spectral measurements. In detail, the sample tablets were excited by the LD and the signals were collected by a focal lens whose focus position was the entrance slit of the spectrometer. The axis of the focal lens was leaned against the pump beam at 30° and intersected with the pump beam at the front surface of the sample. A filter to reflect the 808-nm pump beam but having high transmittance at longer wavelength was employed in front of the entrance slit of the spectrometer. The integral time was aptly selected according to the photoluminescence intensity, with the spectral resolution of 2 nm for all photoluminescence measurements.

Preparation of $Er_2(BDC)_3(DMF)_2(H_2O)_2 \cdot H_2O$ (1). A mixture of $Er(NO_3)_3 \cdot 5H_2O$ (0.0512 g, 0.115 mmol) and H_2BDC (0.0290 g, 0.175 mmol) in a solution containing DMF (3 mL), C_2H_5OH (3 mL), and H_2O (2 mL) in a sealed vial (20 mL) was heated at 80 °C for 24 h. Light-purple crystals of **1** were filtered, dried in air, and collected in ca. 65% yield [on the basis of $Er(NO_3)_3 \cdot 5H_2O$]. Anal. Calcd for **1**, $C_{30}H_{32}Er_2N_2O_{17}$: C, 35.08; H, 3.14; N, 2.73. Found: C, 34.90; H, 2.75; N, 2.48. $Er_2(BDC)_3$ (**1a**) was formed by heating compound **1** under vacuum at 140 °C overnight. Anal. Calcd for **1a**, $C_{24}H_{12}Er_2O_{12}$: C, 34.86; H, 1.46. Found: C, 34.72; H, 1.81.

Preparation of $Er_2(BDC\text{-}F_4)_3(DMF)(H_2O) \cdot DMF$ (2). A mixture of $Er(NO_3)_3 \cdot 5H_2O$ (0.0497 g, 0.112 mmol) with $H_2BDC\text{-}F_4$ (0.0400 g, 0.168 mmol) in a solution containing DMF (3 mL), C_2H_5OH (3 mL), and H_2O (3 mL) in a sealed vial (20 mL) was heated at 80 °C for 24 h. Light-purple crystals of **2** were filtered, dried in air, and collected in ca. 43% yield [on the basis of $Er(NO_3)_3 \cdot 5H_2O$]. Anal. Calcd for **2**, $C_{30}H_{16}Er_2F_{12}N_2O_{15}$: C, 29.85; H, 1.34; N, 2.32. Found: C, 29.66; H, 1.06; N, 1.98. $Er_2(BDC\text{-}F_4)_3(DMF) \cdot DMF$ (**2a**) was formed by heating compound **2** under vacuum at 140 °C overnight. Anal. Calcd for **2a**, $C_{30}H_{14}Er_2F_{12}N_2O_{14}$: C, 30.30; H, 1.19; N, 2.36. Found: C, 30.33; H, 1.22; N, 2.43.

Single-Crystal Structure Determinations. Crystals of **1** and **2** were transferred from a crystallization vessel to a drop of polybutane oil on a microscope slide. Using a nylon loop, a single crystal was than picked and mounted on a Bruker X8 APEX II diffractometer (Mo radiation) in a cold (−100 °C) N_2 stream. Data collection and reduction were done using the Bruker Apex2 software package. The structures were solved by direct methods and subsequent difference Fourier techniques (*SHEXLTL*). All non-H atoms were refined anisotropically. H atoms were added to a model in their geometrically ideal positions. Crystallographic data and structural refinements for **1** and **2** are summarized in Table 1.

(2) Chen, B.; Ockwig, N. W.; Millward, A. R.; Contreras, D. S.; Yaghi, O. M. *Angew. Chem., Int. Ed.* **2005**, *44*, 4745. Chen, B.; Liang, C.; Yang, J.; Contreras, D. S.; Clancy, Y. L.; Lobkovsky, E. B.; Yaghi, O. M.; Dai, S. *Angew. Chem., Int. Ed.*, **2006**, *45*, 1390. Chen, B.; Ma, S.; Zapata, F.; Lobkovsky, E. B.; Yang, J. *Inorg. Chem.* **2006**, *45*, 5718.
(3) Reineke, T. M.; Eddaoudi, M.; Fehr, M.; Kelley, D.; Yaghi, O. M. *J. Am. Chem. Soc.* **1999**, *121*, 1651. Liu, W. S.; Jiao, T. Q.; Li, Y. Z.; Liu, Q. Z.; Tan, M. Y.; Wang, H.; Wang, L. F. *J. Am. Chem. Soc.* **2004**, *126*, 2280. Zhao, B.; Chen, X.-Y.; Cheng, P.; Liao, D.-Z.; Yan, S.-P.; Jiang, Z.-H. *J. Am. Chem. Soc.* **2004**, *126*, 15394. Chandler, B. D.; Cramb, D. T.; Shimizu, G. K. H. *J. Am. Chem. Soc.* **2006**, *128*, ASAP.
(4) Guo, X. D.; Zhu, G. S.; Fang, Q. R.; Xue, M.; Tian, G.; Sun, J. Y.; Li, X. T.; Qiu, S. L. *Inorg. Chem.* **2005**, *44*, 3850. Guo, X. D.; Zhu, G. S.; Sun, F. X.; Li, Z. Y.; Zhao, X. J.; Li, X. T.; Wang, H. C.; Qiu, S. L. *Inorg. Chem.* **2006**, *45*, 2581.
(5) Slooff, L. H.; Van Blaaderen, A.; Polman, A.; Hebbink, G. A.; Klink, S. I.; van Veggel, F. C. J. M.; Reinhoudt, D. N.; Hofstraat, J. W. *J. Appl. Phys.* **2002**, *91*, 3955.
(6) Wang, H. S.; Qian, G. D.; Wang, M. Q.; Zhang, J. H.; Luo, Y. S. *J. Phys. Chem. B* **2004**, *108*, 8084. Wang, H. S.; Qian, G. D.; Wang, Z. Y.; Zhang, J. H.; Luo, Y. S.; Wang, M. Q. *J. Lumin.* **2005**, *113*, 214.
(7) Banerjee, S.; Huebner, L.; Romanelli, M. D.; Kumar, G. A.; Riman, R. E.; Emge, T. J.; Brennan, J. G. *J. Am. Chem. Soc.* **2005**, *127*, 15900.
(8) Beeby, A.; Faulkner, S. *Chem. Phys. Lett.* **1997**, *266*, 116.
(9) Hasegawa, Y.; Murakoshi, K.; Wada, Y.; Yanagida, S.; Kim, J.-H.; Nakashima, N.; Yamanaka, T. *Chem. Phys. Lett.* **1996**, *248*, 8.
(10) Wada, Y.; Okubo, T.; Ryo, M.; Nakazawa, T.; Hasegawa, Y.; Yanegida, S. *J. Am. Chem. Soc.* **2000**, *122*, 8583.
(11) Mancino, G.; Ferguson, A. J.; Beeby, A.; Long, N. J.; Jones, T. S. *J. Am. Chem. Soc.* **2005**, *127*, 524.

Table 1. Crystal and Structure Refinement Data for **1** and **2**

compound	$Er_2(BDC)_3(DMF)_2(H_2O)_2 \cdot H_2O$ (**1**)	$Er_2(BDC\text{-}F_4)_3(DMF)(H_2O) \cdot DMF$ (**2**)
formula	$C_{15}H_{16}ErNO_{8.5}$	$C_{30}H_{16}Er_2F_{12}N_2O_{15}$
M_r	513.55	1206.97
cryst size (mm^3)	0.25 × 0.15 × 0.05	0.30 × 0.20 × 0.15
cryst syst	triclinic	triclinic
space group	$P\bar{1}$	$P\bar{1}$
a (Å)	8.5247(3)	11.6710(18)
b (Å)	10.2004(3)	11.8916(19)
c (Å)	10.8898(4)	14.305(2)
α (deg)	63.722(2)	110.633(7)
β (deg)	71.281(2)	99.920(6)
γ (deg)	81.148(2)	101.351(6)
V ($Å^3$)	804.08(5)	1757.4(5)
T (K)	173	173
D_{calcd} ($Mg\ m^{-3}$)	2.084	2.281
Z	2	2
F(000)	488	1148
μ(Mo Kα) (mm^{-1})	5.264	4.882
no. of reflns collected/ unique (R_{int})	35405/9658 (0.0258)	34644/9527 (0.0270)
data/params	9658/275	9527/558
R1[a]	0.0198	0.0266
wR2[b]	0.0440	0.0768
GOF	1.079	1.129

[a] $R1 = \sum(|(|F_o| - |F_c|)|/\sum|F_o|$. [b] $wR2 = [\sum w(F_o^2 - F_c^2)^2/\sum w(F_o^2)^2]^{1/2}$.

Results and Discussion

Compounds **1** and **2** were synthesized by solvothermal reactions in mixed solvents of DMF, ethanol, and H_2O at a temperature of 80 °C for 24 h. The formulas of the compounds were determined by single-crystal XRD studies, and the phase purity of the bulk materials was independently confirmed by elemental microanalysis, PXRD, and TGA.

Crystal Structure Descriptions of 1 and 2. As shown in Figure 1a, the structure of **1** consists of binuclear Er clusters as building blocks bridged by two bis-monocarboxylates from two BDCs. Each Er is further coordinated by four O atoms from two bidentate chelating carboxylates of two BDCs, one terminal DMF, and one terminal H_2O in a distorted square-antiprism geometry. These binuclear Er clusters can be topologically viewed as octahedral nodes, which are connected by six BDCs to form a three-dimensional (3D) distorted primitive cubic framework (Figure 1b). When the binuclear Er cluster is simplified as a Po atom, the overall structure of **1** is a pair of identical α-Po nets of $Er_2(BDC)_3(DMF)_2(H_2O)_2$ that are mutually interpenetrated with each other to form a doubly interpenetrating 3D framework (Figure 1c). A space-filling model of the structure **1** is shown in Figure 1d, indicating that the pores are filled by another identical framework and coordinated solvent molecules.

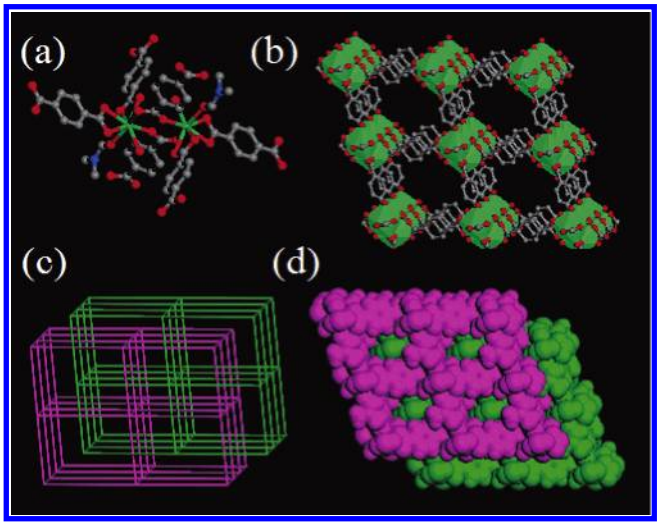

Figure 1. Structure of **1** showing (a) the coordination geometry of the secondary building unit of a $Er_2(BDC)_3(DMF)_2(H_2O)_2$ cluster, (b) its primitive cubic α-Po net (H atoms are omitted for clarity; Er, light green; N, blue; O, red; C, gray), (c) a schematic illustration of the doubly interpenetrating frameworks in purple and green [center of the $Er_2(BDC)_3(DMF)_2(H_2O)_2$ cluster as the Po node], and (d) its corresponding space-filling representation indicating the formation of a condensed structure.

The structure of **2** is a rod-packing framework[12] consisting of two types of Er atoms, both in distorted square-antiprism geometries, which are bridged by two bis-monocarboxylates from two BDC-F_4 linkers. As shown in Figure 2a, Er1 (right) is further coordinated by five O atoms from four BDC-F_4 linkers and one H_2O, while Er2 (left) is fulfilled by five O atoms from four BDC-F_4 and one DMF. Each Er atom is further connected with the central symmetrically related Er atom by four BDC-F_4 linkers, forming a one-dimensional (1D) rod (Figure 2b,c). The space-filling model indicates that the pores in this framework are mainly occupied by coordinated solvent molecules, and there exist 1D tiny pores along the a axis that are filled with free DMF molecules (Figure 2d).

Although **1** and **2** have quite different crystal structures, the emissive Er ions/unit volume of 1.24 Er^{3+}/1000 $Å^3$ in **1** is only slightly higher than that of 1.14 Er^{3+}/1000 $Å^3$ in **2**. Their structural diversity is partly attributed to the different spatial arrangement of the organic linkers BDC and BDC-F_4 in **1** and **2**, respectively. The carboxylate group in **1** is almost coplanar with the phenyl plane of the BDC linker, while the carboxylate group in **2** significantly deviates from

(12) Rosi, N. L.; Kim, J.; Eddaoudi, M.; Chen, B.; O'Keeffe, M.; Yaghi, O. M. *J. Am. Chem. Soc.* **2005**, *127*, 1504.

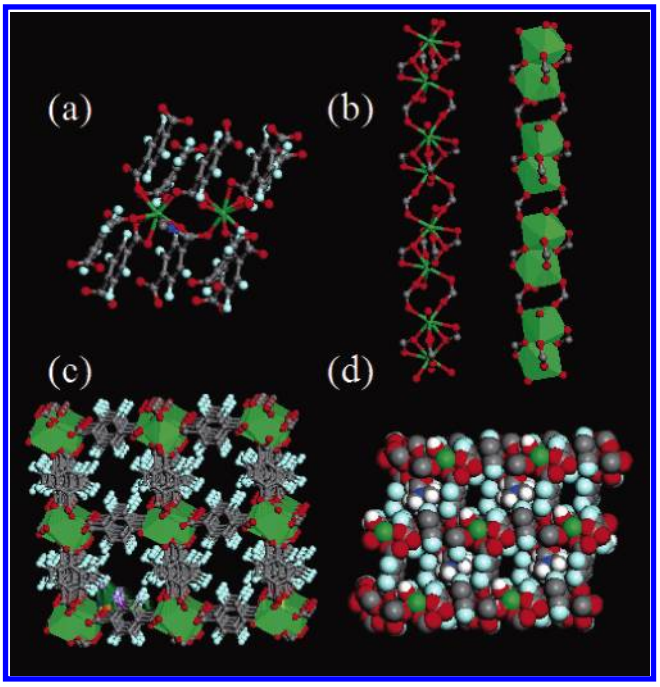

Figure 2. Structure of **2** showing (a) the coordination geometry of the binuclear $Er_2(BDC\text{-}F_4)_3(DMF)(H_2O)$ fragment, (b) a 1D infinite secondary building unit with ball-and-stick representation (left) and with Er atoms shown as polyhedra (right), (c) a 3D MOF viewed along the 1D $Er_2(CO_2)_6$ rod (DMF and H_2O molecules are omitted for clarity), and (d) a space-filling representation viewed along the *a* axis (uncoordinated DMF molecules are omitted for clarity; Er, light green; F, light cyan; N, blue; O, red; C, gray).

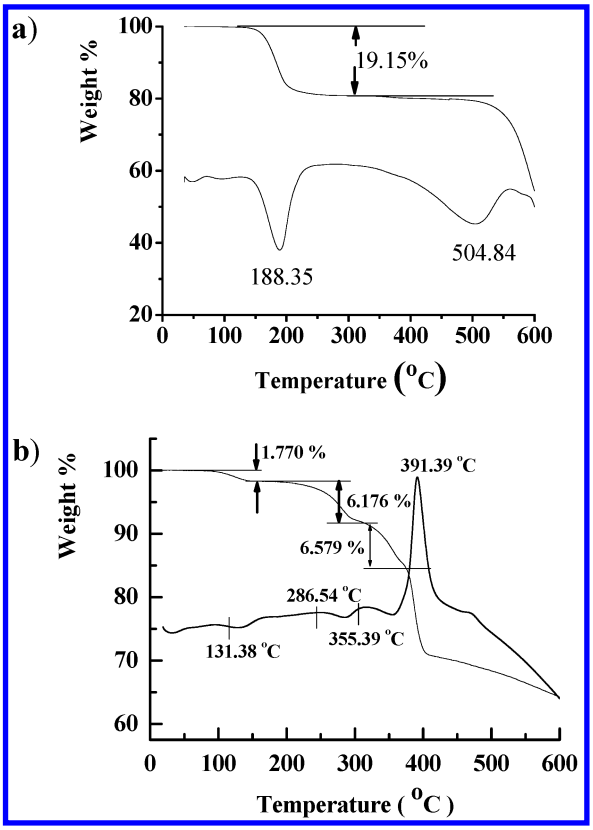

Figure 3. TGA−DSC diagrams of (a) **1** and (b) **2**.

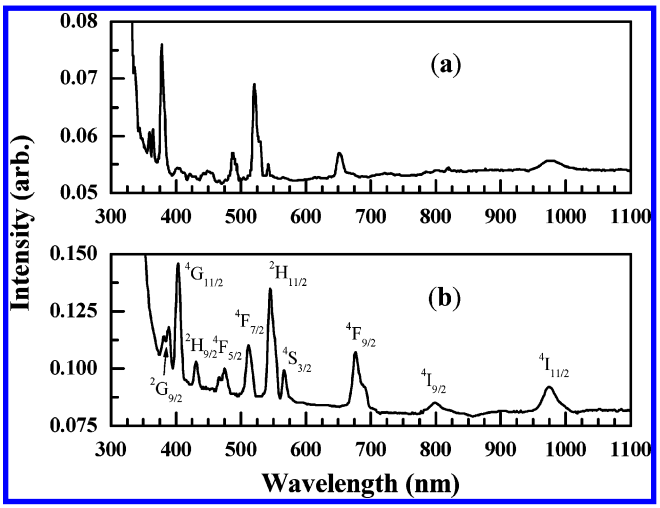

Figure 4. UV−vis−near-IR absorption spectra of (a) **1** and (b) **2**, respectively.

the phenyl plane of the BDC-F_4 linker because of the stronger repulsion between F and carboxylate.

TGA−DSC Study. TGA−DSC studies indicated that compound **1** starts losing solvent molecules at a temperature of 135 °C and the desolvated compound **1a** is stable up to about 480 °C (calcd solvent loss (2DMF + 3H_2O), 19.48%; exptl, 19.15%; Figure 3a). Compound **2** gradually loses H_2O (calcd, 1.49%; exptl, 1.77%), free DMF (calcd, 6.05%; exptl, 6.18%), and coordinated DMF (calcd, 6.05%; exptl, 6.58%) at elevated temperatures (Figure 3b).

UV−Vis−Near-IR Spectroscopy and Luminescence Properties. Compounds **1** and **2** exhibit well-resolved UV−vis−near-IR absorption spectra (Figure 4). The strong absorption below 350 nm is ascribed to the organic linker's $\pi-\pi$ transitions, while 10 absorption bands above 350 nm can be readily assigned to the corresponding electronic transitions of the Er^{3+} ion from the ground state $^4I_{15/2}$ to the excited states $^4I_{13/2}$, $^4I_{11/2}$, $^4I_{9/2}$, $^4F_{9/2}$, $^4S_{3/2}$, $^2H_{11/2}$, $^4F_{7/2}$, $^4F_{5/2}$, $^2H_{9/2}$, $^4G_{11/2}$, and $^2G_{9/2}$.

The fluorescence properties of the compounds were studied under excitation of an 808-nm band using LD as the light source. No fluorescence was detected from the as-synthesized compounds **1** and **2** at room temperature. This is mainly because of the quenching effect of high-energy C−H and/or O−H oscillators from free and coordinated H_2O and DMF solvent molecules. To minimize the solvents' quenching effect, the as-synthesized compounds were activated under vacuum at 140 °C overnight to form the desolvated solid **1a** and the partially desolvated solid **2a** for near-IR−luminescence studies, which were also carried out under the excitation of an 808-nm band using LD as the light source (Figure 5). Before their luminescence properties were examined, compounds **1a** and **2a** were characterized by elemental analysis, IR, and PXRD. **1a** is a poor crystalline solid whose PXRD is significantly broadened and different from that of **1**. IR spectra of **1a** show that DMF C═O stretches at 1651 cm^{-1} completely disappear and carboxylate C═O stretches and phenyl vibrations match well with those of **1**. **1a** is stable in air, presumably a condensed solid by further coordination of some carboxylate O atoms to Er ions. **2a** has the same

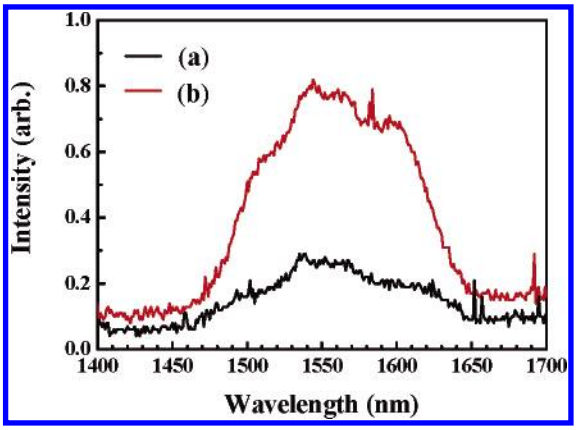

Figure 5. Near-IR−fluorescence spectra of (a) **1a** and (b) **2a** excited at 808 nm by a LD.

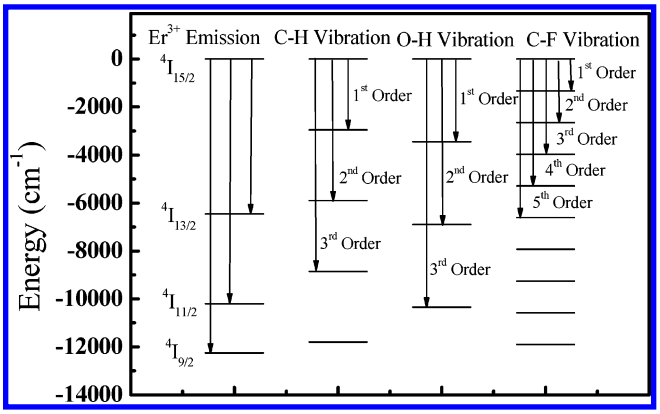

Figure 6. Schematic representation of the vibrational quenching of the $^4I_{13/2}$ emission of Er^{3+} by the vibrational modes of CH, OH, and CF functional groups.

structure as **2**, as shown in its PXRD, which is slightly different from that of **2**, and IR spectra, which are almost identical with that of **2**. It is of special interest to note that the fluorescent emission intensity of **2a** at about 1.55 μm, which is attributed to the $^4I_{13/2} \rightarrow {}^4I_{15/2}$ transition of a Er^{3+} ion, is significantly enhanced and is about 3 times higher than that of **1a**. Because **2a** still contains a certain amount of DMF solvent molecules, which can reduce the luminescence intensity, we speculate that the fluorination can greatly improve the quantum yield of the $^4I_{13/2} \rightarrow {}^4I_{15/2}$ transition in erbium−organic framework materials.

The mechanisms for such an improvement in fluorescent erbium−organic framework materials are clearly illustrated in Figure 6, in which the energy level diagrams of the Er^{3+} ion, C−H (2950 cm^{-1}) and C−F (1220 cm^{-1}) vibrations, are presented. It can be seen that the second-order C−H bond vibrational frequencies (5900 cm^{-1}) are almost in resonance with the emission bands of the Er^{3+} ion at 1.5 μm ($^4I_{13/2} \rightarrow {}^4I_{15/2}$), while only the fifth-order C−F bond vibrational frequencies (6100 cm^{-1}) can approach in resonance with such an emission transition; thus, the effect of the C−F vibration on the fluorescence quenching of the Er^{3+} ion emission is much lower than that of the C−H vibration. By making use of fluorinated organic linker BDC-F_4 instead of BDC, such a fluorescence quenching effect is much reduced and minimized, leading to a higher luminescence intensity of compound **2a** than of **1a**.

It is assumed that the luminescence intensity of Er−BDC-F_4 frameworks can be further enhanced by eliminating the solvents' quenching effect. Because it is quite difficult to further activate compound **2a** at elevated temperature to form a new stable solid because of its low thermal stability, we plan to incorporate ancillary electron-rich organic ligands instead of solvent molecules to saturate the Er^{3+} coordination sites. Such efforts have been ongoing to target more promising near-IR emissive Er−BDC-F_4 framework solids for their potential applications in sensing and optics.

Acknowledgment. This work was supported by the University of Texas−Pan American (UTPA) through a Faculty Research Council award (B.C.), in part by the Welch Foundation Grant BG-0017 to the Department of Chemistry at UTPA. The authors also gratefully acknowledge the financial support for this work from the National Natural Science Foundation of the People's Republic of China (Grant 50532030) and the Foundation for the Author of National Excellent Doctoral Dissertation of the People's Republic of China (Grant 200134).

Supporting Information Available: X-ray data in CIF format, PXRD patterns, and IR spectra. This material is available free of charge via the Internet at http://pubs.acs.org.

IC060568U